Role of nanostructured aggregation of chitosan derivatives on [5-methionine]enkephalin affinity

Federica Aiello[a], Federica Balzano[a], Luca Carpita[a], Angela Fabiano[b], Ylenia Zambito[b], Gloria Uccello Barretta[a]*

[a] *Università di Pisa, Dipartimento di Chimica e Chimica Industriale, Via Giuseppe Moruzzi 13, 56124 Pisa, Italy.*
Email addresses: federica.aiello87@gmail.com, federica.balzano@unipi.it, lucarpita@hotmail.it, gloria.uccello.barretta@unipi.it
[b] *Università di Pisa, Dipartimento di Farmacia, Via Bonanno Pisano 6, 56126 Pisa, Italy. Email addresses: angyfab@gmail.com, ylenia.zambito@unipi.it*

---

* Corresponding author: Tel: +39 050 2219232; fax +39 050 2219260 (G. Uccello Barretta)

17

Abstract

Affinities of quaternary ammonium-chitosan conjugates, their thiolated derivatives and corresponding nanostructured aggregates towards the hydrophilic drug [5-methionine]enkephalin were compared by Nuclear Magnetic Resonance (NMR) spectroscopic methods based on proton selective relaxation rate measurements. Nanoaggregates showed enhanced drug affinity in comparison with corresponding polymers, especially in the case of thiolated systems.

24

27

1. Introduction

Nanoparticulate systems have attracted increasing attention, in consideration of their strong technological impact. In pharmaceutical and biomedical fields, these systems may be exploited also for prolonging drug residence at the adsorption site, thus allowing to reduce the frequency of dosing and minimizing the side effects (Düunhaupt et al., 2011; Sakuma et al., 2002). Since drugs are preferentially administered orally, by inhalation or transdermally, it is very important to find carriers endowed with good mucoadhesivity. For this reason, mucoadhesive, biocompatible and biodegradable polymers have usually been chosen as the starting materials, among which chitosan (Ch) and its derivatives play a significant role (Agnihotri, Mallikarijuna & Aminabhavi, 2004).

Quaternized chitosans (QA-rCh60, Fig. 1), thiolated derivatives (QA-rCh60-SH, Fig. 1) and corresponding nanoparticulate structures (NP-QA-rCh60 or NP-QA-rCh60-SH, Zambito, Uccello-Barretta, Zaino, Balzano, & Di Colo, 2006; Zambito et al., 2009; Zambito, Felice, Fabiano, Di Stefano, & Di Colo, 2013) revealed good effectiveness in the delivery of mainly lipophilic drugs, as

41 demonstrated by employing dexamethasone 21-phosphate as interaction probe (Uccello-Barretta et

42 al., 2014; Fabiano, Chetoni, & Zambito, 2015). In particular, the use of Nuclear Magnetic

43 Resonance (NMR) spectroscopy allowed the detection of intermolecular interactions between the

44 drug and the macromolecules (Uccello-Barretta et al., 2014), by exploiting the high sensitivity of

45 relaxation parameters of NMR active nuclei to complexation phenomena (Neuhaus & Williamson,

46 1989; Valensin, Sabatini, & Tiezzi, 1986).
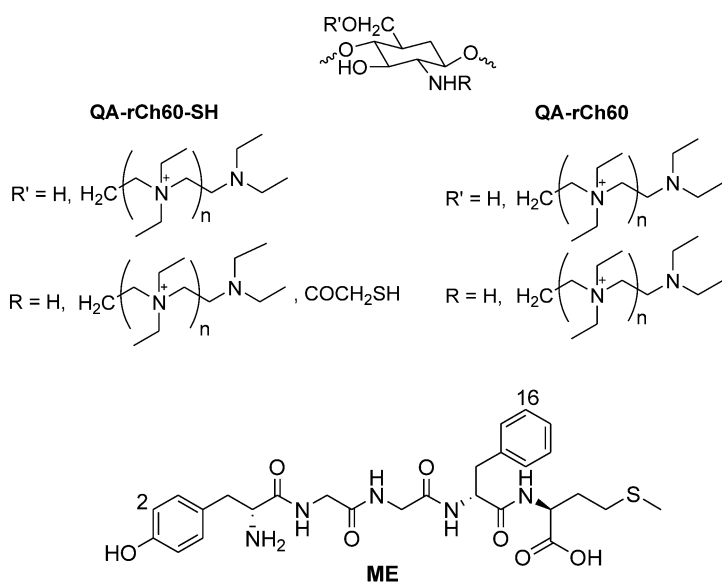
47

48 **Fig.1**. Chemical structures of quaternarized chitosan derivatives (Cl⁻ counterion) employed for the preparation of

49 nanoparticles and of [5-methionine]enkephalin (ME) with numbering scheme for NMR analysis

50

51 Recently, the protective effectiveness in ophthalmic applications of nanoaggregated derivatized

52 chitosans towards [5-methionine]enkephalin (ME, Fig. 1), a pentapeptide of the enkephalin family,

53 has been demonstrated (Fabiano et al., 2015); also an enhanced mean drug residence time was

54 achieved. Peptide drugs constitute, in fact, an important class of bioactive systems, which, however,

55 need to be protected against degradation processes (Kashi & Lee, 1986; Hämäläinen, Ranta,

56 Auriola, & Urtti, 2000) that can occur in the pre-corneal area.

57 In this study, NMR spectroscopy has been then exploited as a non-invasive investigation tool for

58 detecting and comparing the affinity of ME for both quaternary ammonium-chitosan conjugates

(thiolated and non-thiolated) and for corresponding nanoparticles, in order to point out the importance of the nanoparticulate aggregation in the interaction with the hydrophilic drug. The mucoadhesive properties of both polymers and nanoparticles were detected in ternary mixtures containing bovine submaxillary mucin (BSM). In addition, the release properties of loaded nanoparticles were investigated by performing quantitative NMR experiments.

2. Materials and methods

2.1. Materials

Bovine submaxillary mucin (BSM), [5-methionine]enkephalin (ME) and phosphate buffer (pH 7.4) were purchased from Sigma Aldrich (St. Louis, Missouri, United States). Deuterated water (D_2O) was purchased from Deutero GmbH (Kastellaun, Germany). Hyaluronic acid (HA), MW 950 kDa was purchased from (Contipro, Dolní Dobrouc,ˇ Czech Republic); chitosan minimum 90% deacetylated from shrimp shell (Chitoclear FG90, Primex, Drammen, Norway). The commercial chitosan had an average viscometric molecular weight of 590 kDa and a deacetylation degree, determined by IR or NMR, of 90% or 82% (Zambito et al., 2006). Its MW was reduced by oxidative depolimerisation (see, e.g., Janes & Alonso, 2003; Mao et al., 2004), to obtain rCh (viscometric MW, 32 kDa). The MW of HA was reduced by acid degradation, according to Liu, Luo, Roberts, & Prestwich (2002), to obtain rHA (viscometric MW 470 kDa). The viscometric MWs of rCh and rHA were determined by an Ostwald U-tube capillary viscometer (Cannon-Fenske series ASTM 75), following the procedure reported by Khalid, Ho, Agnely, Grossiord, & Couarraze (1999) for rCh in 0.1 M acetic acid/0.2 M NaCl, and that reported by Tadmor, Chen, & Israelachvili (2002) for rHA in 0.1 M NaCl. The quaternary ammonium-rCh conjugate was synthesized by reacting diethylaminoethyl chloride hydrochloride with rCh, through a procedure similar to that described by Zambito et al. (2006) and Zambito, Zaino, Uccello-Barretta, Balzano, & Di Colo (2008), keeping the pH at 8 and controlling the temperature at 60 °C (product code, QA-rCh60).

84   Thiolation of QA-rCh60 was achieved by the attachment of thioglycolic acid (TGA) to

85   unsubstituted primary amino groups still present on the QA-rCh60 chains, via formation of amide

86   bonds mediated by EDAC (Kast & Bernkop-Schnürch, 2001). QA-rCh60 and QA-rCh60-SH were

87   the same synthesized in a previous work by Zambito, Felice, Fabiano, Di Stefano, & Di Colo

88   (2013), while the relevant medicated NP were prepared as described by Fabiano et al. (2015) with

89   an efficiency of ME encapsulation of about 30%.

90

91   *2.2.   NMR measurements*

92   NMR measurements were performed on a Varian INOVA600 spectrometer operating at 600 MHz

93   and 150 MHz for ^{1}H and ^{13}C nuclei. The temperature was controlled to $\pm$ 0.1°C. DOSY (Diffusion

94   Ordered SpectroscopY) experiments were carried out by using a stimulated echo sequence with

95   self-compensating gradient schemes and 64K data points. Typically, g was varied in 20 steps (2-32

96   transients each), Δ and δ were optimized in order to obtain an approximately 90-95% decrease in

97   the resonance intensity at the largest gradient amplitude. The baselines of all arrayed spectra were

98   corrected prior to processing the data. After data acquisition, each FID was apodized with 1.0 Hz

99   line broadening and Fourier transformed. The data were processed with the DOSY macro

100 (involving the determination of the resonance heights of all the signals above a pre-established

101 threshold and the fitting of the decay curve for each resonance to a Gaussian function) to obtain

102 pseudo two-dimensional spectra with NMR chemical shifts along one axis and calculated diffusion

103 coefficients along the other. Gradient amplitudes in DOSY experiments have been calibrated by

104 using a standard sample of D_2O 99% (19 x 10^{-10} m^2s^{-1}). The spin-lattice selective relaxation times

105 were measured in the initial rate approximation (Freeman & Wittekoek, 1969) by using the

106 inversion recovery pulse sequence $(180°-\tau-90°-t)_n$ and by applying a selective π-pulse at the

107 selected frequency and a relaxation delay of 15 s. Release studies of loaded nanoparticles were

108 performed by recording ^{1}H NMR quantitative spectra, with the following acquisition parameters:

109 pulse width = 5.5 μs (45° pulse), 5 s relaxation delay, 48 transients. The spectra were acquired each

hour, and the concentration of the drug was calculated on the selected signal by the qEstimate software (Agilent) and by comparing its integrated area to that of a sample of drug at known concentration.

^{1}H and ^{13}C NMR characterization data of ME, in the selected experimental conditions (pH=7.4 phosphate buffer, 25 °C, D_2O, 2.5 mM) are reported in the Supplementary Material.

3. Results and Discussion

3.1. Affinity studies

Before facing the investigation regarding ME to polymers affinities, DOSY experiments were exploited for probing potential viscosity changes, which could have affected the interpretation of affinity data. As a matter of fact, decreases of the translational diffusion coefficient are expected as the consequence of viscosity increase, which could occur in solutions containing the polymers. In particular all our NMR samples were added by a standard solution (50 μL) containing tetramethylsilane (TMS) in DMSO (7% v/v) and diffusion coefficient of TMS was measured. In all cases no changes of TMS diffusion coefficient were detected, thus allowing us to rule out viscosity effects. In addition the diffusion coefficients of ME and acetate counterion were remarkably differentiated (3.0 x 10^{-10} m^2s^{-1} and 7.6 x 10^{-10} m^2s^{-1} for ME and acetate respectively), thus allowing us to exclude the formation of tight ME/acetate ion pairs which could once again affect the binding processes.

We investigated drug-macromolecule interactions in mixtures containing ME and polymers or their empty NPs, with the aim to highlight the effect of supramolecular assembly in nanoparticulate forms on binding processes. A very high drug/macromolecule ratio (from 20:1 to 100:1 or greater) is requested in order to obtain a detectable NMR signal for the drug. In fast-exchange conditions, the observed parameter represents the weighted average of its value in the bound (P_b) and free (P_f) states ($P = x_f P_f + x_b P_b$, where x_f and x_b are the molar fractions of the free and bound states,

respectively). Thus only NMR parameters undergoing a sharp change as the consequence of the interaction can be usefully exploited. Among the available observable NMR parameters, proton selective relaxation rates ($R_1^{ms} = 1/T_1^{ms}$, where T_1^{ms} is the measured mono-selective relaxation time) were selected for affinity studies, since they are highly responsive to the slowing down of molecular motions of drugs, due to binding interactions with macromolecules (Uccello-Barretta et al., 2014; Neuhaus & Williamson, 1989; Valensin et al., 1986). Indeed, when the molecular motion of the drug is slowed down to the $\omega^2\tau_c^2 \gg 1$ (ω = Larmor frequency, τ_c = reorientational correlation time) region as a consequence of the interaction with the macromolecule, mono-selective relaxation rates show a sharp increase, whereas the non-selective relaxation rates reach a maximum for $\omega^2\tau_c^2 \cong 1$ and then decrea with further increasing $\omega^2\tau_c^2$.

R_1^{ms} can be then obtained by selectively inverting one selected resonance and leaving unperturbed the others (Fig. 2) and by following the recovery of the magnetization to equilibrium. Errors in the relaxation times values were always less than 1% and, hence, changes measured could be unequivocally attributed to binding effects, once excluded viscosity changes by means of DOSY measurements.
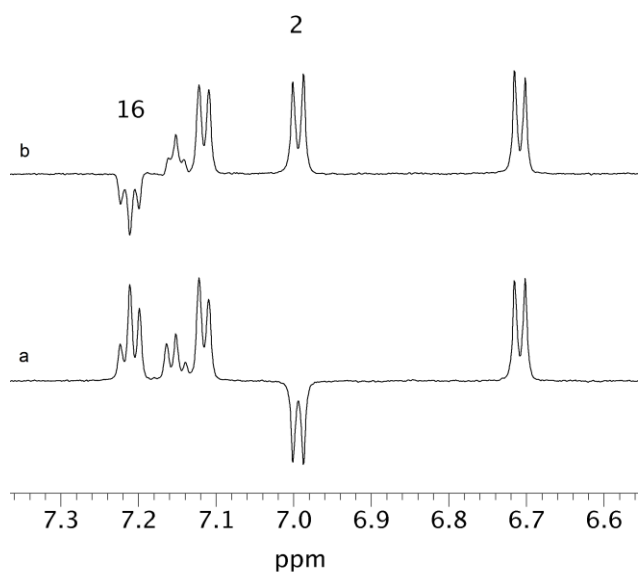
Fig. 2. Mono-selective inversion of (a) H-2 and (b) H-16 resonances of ME for relaxation measurements.

152 Aromatic protons H2 of tyrosine and H16 of phenylalanine of ME (Fig. 1) were selectively

153 inverted, because no superimposition with polymer signals was observed (Fig. S1, Supplementary

154 Material). The drug was employed at a concentration of 2.5 mM (1.43 mg/mL).

155 The mono-selective relaxation rates of ME nuclei were detected for each mixture drug/polymer or

156 drug/nanoparticle (R_{mix}) and compared with the values of free ME (R_f), thus obtaining the

157 normalized mono-selective relaxation rates (Eq. 1), which only depends on the strength of the

158 interaction and, hence, on drug to polymer affinity:

159 $$\Delta R/R_f = \left(R_{mix} - R_f\right)/R_f \qquad \text{(Eq. 1)}$$

160 Binary mixtures containing an equal amount (weight) of drug and polymers (1.43 mg/mL) were

161 firstly analyzed, but in these experimental conditions negligible variations in normalized relaxation

162 rates of ME protons were detected (Table 1). In order to favor the interaction, the amount of

163 polymer was then increased till to reach 10 to 1 and 20 to 1 polymer to ME w/w ratios. The non-

164 thiolated polymer demonstrated an enhanced propensity to interact with the drug at the higher w/w

165 ratios (Table 1), being tyrosine residue (H2 protons) involved in a larger extent with respect to the

166 molecular portion bearing Phe residue (H16 protons).

Table 1- Normalized mono-selective relaxation rates ($\Delta R/R_f$) of selected protons of ME (1.43 mg/mL, 600 MHz, D_2O pH 7.4, 25 °C) in binary mixtures with polymers at different ME/polymer w/w ratios (reported in parenthesis) or nanoparticles (containing 1.43 mg/mL of QA-rCh60 or QA-rCh60-SH) and in binary and ternary mixtures with BSM (10 mg/mL).

	$\Delta R/R_f$	
	H2	H16
ME/QA-rCh60 (1:1)	0.03	0.02
ME/QA-rCh60 (1:10)	0.14	0.09
ME/QA-rCh60 (1:20)	0.31	0.11
ME/QA-rCh60-SH (1:1)	0.03	0.02
ME/QA-rCh60-SH (1:10)	0.06	0.07
ME/QA-rCh60-SH (1:20)	0.09	0.07
ME/NP-QA-rCh60	0.86	0.41
ME/NP-QA-rCh60-SH	1.97	0.86
ME + BSM	6.17	5.64
ME/NP-QA-rCh60 + BSM	8.17	7.39
ME/NP-QA-rCh60-SH + BSM	9.00	9.50

167

The nanoparticulate arrangement of both chitosan derivatives favors the interaction with the drug, since the normalized relaxation rates of aromatic protons of ME underwent a more sensitive increase in binary mixtures containing empty nanoparticles in place of polymers (1:1 w/w, Table 1), thus highlighting the importance of the supramolecular assembly in the interaction.

Once again, the interaction between ME and NPs mainly involves terminal tyrosine residue of the pentapeptide (Table 1). Interestingly, a stronger interaction between ME and thiolated nanoparticles was pointed out. By contrast the pentapeptide showed greater affinity for non-thiolated polymer than it did for thiolated one (Table 1). It is noteworthy that largely hydrophobic dexamethasone 21-phosphate showed enhanced affinity for thiolated polymers and non-thiolated nanoparticles (Uccello-Barretta et al., 2014).

3.2. Mucoadhesive properties

In order to obtain information about the mucoadhesive properties of chitosan nanoparticles, ternary mixtures containing bovine submaxillary mucin (BSM) were considered.

In ternary mixtures containing BSM and the nanoaggregates (Table 1), the normalized changes of relaxation rates were not additive with respect to the values detected in corresponding binary mixtures (ME/BSM and ME/NPs, Table 1). This data demonstrate the occurrence of NP/BSM interactions, responsible for an increase of ME affinity for NP/BSM supramolecular aggregates with respect to NPs or BSM.

3.3. Release analysis

ME release from loaded nanoparticles (1.57 mM ME) in water solution was followed directly into the NMR tube over 24 h. The released amount was calculated on the basis of the changes of H2 proton integrated area, by using as reference for the quantitative analysis a sample of ME with known concentration. In Table 2 the percentage of free drug found in each sample is reported.

Table 2- Percentage of ME released from loaded nanoparticles (600 MHz, D_2O pH = 7.4, 25 °C)

	ME (mM)	
	t_0	24 h
NP-QA-rCh60	63 %	64 %
NP-QA-rCh60-SH	71 %	71 %

Since the encapsulation efficiency was about 30% (Fabiano et al., 2015) and ME unencapsulated had not been removed from the NP, NMR data (Table 2) demonstrates that ME amounts at t_0 is in agreement with the amount of unencapsulated ME and remains nearly unchanged after 24 hours. These release data are in agreement with the dialysis experiments performed by Fabiano et al. (2015), which indicated that no release of ME from loaded nanoparticles occurs in the first 24 hours, thus suggesting a very good stability of the corresponding formulations over that time. It is noteworthy that many researchers have reported that chitosan and its derivatives are biodegraded in the body by several enzymes including lysozyme that is present throughout the body (Ren, Yi, Wanga, & Ma, 2005). We hypothesized that drug release could begin with the polymer biodegradation. Therefore the supramolecular systems NP-QA-rCh60 and NP-QA-rCh60-SH are able to shield the peptide from aminopeptidase activity to a significant extent to improve its ocular bioavailability (Fabiano et al., 2015).

4. Conclusions

NMR spectroscopy constitutes a remarkably valuable non-invasive technique for ascertaining several relevant features of pharmaceutical formulations, spanning from drug to polymer or nanoparticles affinities till to mucoadhesive properties and release profiles. Regarding the properties of chitosan derivatives, we demonstrated that hydrophilic drugs have low affinity for derivatized chitosan polymers in comparison to hydrophobic ones (Uccello-Barretta et al., 2014). However, the polymer assembly in nanoaggregated structures strongly affects drug to polymer interaction processes, leading to enhanced affinities. This effect is particularly pronounced in the case of ME/thiolated nanoparticles system. It is noteworthy that, for hydrophobic dexamethasone 21-

phosphate, an enhanced affinity with respect to polymer was pointed out for non-thiolated nanoparticles.

As a clear demonstration of their mucoadhesive properties, both kind of nanoparticles interact with mucin, by forming supramolecular aggregates that favor the interaction with the drug.

Release analysis of loaded nanoparticles, directly performed into the NMR tube, showed that, already at the beginning of release processes, more than half of drug is present as free compound, thus suggesting that, during the encapsulation, a relevant amount of drug strongly interacts with the external surface of the nanoaggregates, accordingly to the effect of supramolecular assembly on interaction processes.

References

Agnihotri, S. A., Mallikarijuna, N. N., & Aminabhavi, T. M. (2004). Recent advances on chitosan-based micro- and nanoparticles in drug delivery. *Journal of Controlled Release*, 100, 5-28.

Dünnhaupt, S., Barthelmes, J., Hombach, J., Sakloetsakun, D., Arkhipova, V., & Bernkop-Schnürch, A. (2011). Distribution of thiolated mucoadhesive nanoparticles on intestinal mucosa. *International Journal of Pharmaceutics*, 408, 191–199.

Fabiano, A., Chetoni, P., & Zambito, Y. (2015). Mucoadhesive nano-sized supramolecular assemblies for improved pre-corneal drug residence time. *Drug Development and Industrial Pharmacy*, 41, 2069–2076.

Freeman, R., & Wittekoek, S. (1969). Selective determination of relaxation times in high resolution NMR. *Journal of Magnetic Resonance*, 1, 238–276.

Hämäläinen, K. M., Ranta, V. P., Auriola, S., & Urtti, A. (2000). Enzymatic and permeation barrier of [D-Ala^2]-Met-enkephalinamide in the anterior membranes of the albino rabbit eye. *European Journal of Pharmaceutical Sciences*, 9, 265–270.

Janes, K. A., & Alonso, M. J. (2003). Depolymerized chitosan nanoparticles for protein delivery: Preparation and characterization. *Journal of Applied Polymer Science*, 88, 2769–2776.

Kashi, S. D., & Lee, V. H. L. (1986). Hydrolysis of enkephalins in homogenates of anterior segment tissues of the albino rabbit eye. *Investigative Ophthalmology & Visual Science*, 27, 1300–1303.

243 Kast, C. E., & Bernkop-Schnürch, A. (2001). Thiolated polymers—thiomers: Development and in vitro evaluation of

244 chitosan–thioglycolic acid conjugates. *Biomaterials*, 22, 2345–2352.

245 Khalid, M. N., Ho, L., Agnely, F., Grossiord, J. L., & Couarraze, G. (1999). Swelling properties and mechanical

246 characterization of a semi-interpenetrating chitosan/polyethylene oxide network. Comparison with a chitosan reference

247 gel. *STP Pharma Sciences*, 9, 359–364.

248 Mao, S., Shuai, X., Unger, F., Simon, M., Bi, D., & Kissel, T (2004). The depolymerization of chitosan: effects on

249 physicochemical and biological properties. *International Journal of Pharmaceutics* 281, 45–54.

250 Neuhaus, D., & Williamson, M. (1989). *The Nuclear Overhauser Effect in Structural and Conformational Analysis*.

251 New York: VCH Publisher.

252 Ren, D., Yi, H., Wanga, W., & Ma, X. (2005). The enzymatic degradation and swelling properties of chitosan matrices

253 with different degrees of N-acetylation. *Carbohydrate Research*, 340, 2403-2410.

254 Sakuma, S., Sudo, R., Suzuki, N., Kikuchi, H., Alashi, M., Ishida, Y., & Hayashi, H. (2002). Behavior of mucoadhesive

255 nanoparticles having hydrophilic polymeric chains in the intestine. *Journal of Controlled Release*, 81, 281-290.

256 Shu, X. Z., Liu, Y., Luo, Y., Roberts, M. C., & Prestwich, G. D. (2002). Disulfide crosslinked hyaluronan hydrogels.

257 *Biomacromolecules*, 3, 1304–1311.

258 Tadmor, R., Chen, N., & Israelachvili, J. N. (2002). Thin film rheology and lubricity of hyaluronic acid solutions at a

259 normal physiological concentration. *Journal of Biomedical Materials Research*, 61 , 514–523

260 Uccello Barretta, G., Balzano, F., Aiello, F., Senatore, A., Fabiano, A., & Zambito, Y. (2014). Mucoadhesivity and

261 release properties of quaternary ammonium–chitosan conjugates and their nanoparticulate supramolecular aggregates:

262 an NMR investigation. *International Journal of Pharmaceutics*, 461, 489-494.

263 Valensin, G., Sabatini, G., & Tiezzi, E. (1986). Determination of zero- and double-quantum relaxation transition

264 probabilities by multiple-selective irradiation methods. In N. Niccolai, G. Valensin (Eds.), *Advanced Magnetic*

265 *Resonance Techniques in Systems of High Molecular Complexity* (pp. 69–76). Boston: Birkhauser Inc.

266 Zambito, Y., Felice, F., Fabiano, A., Di Stefano, R., & Di Colo, G. (2013). Mucoadhesive nanoparticles made of

267 thiolated quaternary chitosan crosslinked with hyaluronan. *Carbohydrate Polymers*, 92, 33-39.

268 Zambito, Y., Fogli, S., Zaino, C., Stefanelli, F., Breschi, M. C., & Di Colo, G. (2009). Synthesis, characterization and

269 evaluation of thiolated quaternary ammonium–chitosan conjugates for enhanced intestinal drug permeation. *European*

270 *Journal of Pharmaceutical Sciences*, 38,112–120.

271 Zambito, Y., Uccello-Barretta, G., Zaino, C., Balzano, F., & Di Colo, G. (2006). Novel transmucosal absorption

272 enhancers obtained by aminoalkylation of chitosan. *European Journal of Pharmaceutical Sciences*, 29, 460–469.

273 Zambito, Y., Zaino, C., Uccello-Barretta, G., Balzano, F., & Di Colo, G. (2008). Improved synthesis of quaternary

274 ammonium-chitosan conjugates (N+-Ch) for enhanced intestinal drug permeation. *European Journal of Pharmaceutical*

275 *Sciences* 33, 343–350.